Thermal Fractionation and Crystallization Enhancement of Silane-Grafted Water-Crosslinked Low-Density Polyethylene

YEONG-TARNG SHIEH, JUI-SHUI CHEN, CHUNG-CHIN LIN

Department of Chemical Engineering, National Yunlin University of Science and Technology, Touliu, Yunlin 640, Taiwan, Republic of China

ABSTRACT: Thermal fractionations performed using differential scanning calorimetry (DSC) to characterize the heterogeneities in molecular structures of low-density polyethylene (LDPE), silane-grafted LDPE (G-LDPE), and silane-grafted water-crosslinked LDPE with gel fractions of 30 and 70 wt % are reported. In regular DSC analyses, LDPE, G-LDPE, and the low gel fraction of crosslinked samples (30 wt %) give one broad endothermic peak at ~110 °C, whereas the high gel fraction of crosslinked samples (70 wt %) give overlapped multiple endothermic peaks in a much broader temperature range. After thermally fractionated in the range 60–145 °C, LDPE, G-LDPE, and the low gel fraction samples give five to six endothermic peaks in the low-temperature range, whereas the high gel fraction samples give nine peaks, with three additional peaks appearing in the high-temperature range. These multiple peaks correspond to fractions of different molecular structures, with the additional peaks for the high gel fraction samples corresponding to the fraction of molecular segments with low or no branching. This fraction of molecular segments is increasingly extruded out of the gel region with increasing gel fraction by crosslinking and leads to an enhancement of crystallization of the sample. This crystallization enhancement behavior is also demonstrated by the X-ray diffraction data and polarized optical micrographs. © 2001 John Wiley & Sons, Inc. J Appl Polym Sci 81: 591–599, 2001

Key words: low-density polyethylene (LDPE); thermal fractionation; grafting; crosslinking; structural heterogeneity; crystallization enhancement

INTRODUCTION

Crosslinking of polyethylene is of considerable practical importance. It extends the range of use by raising the upper temperature limit of application and improves the mechanical properties of this polymer. There are a variety of ways to achieve crosslinking of polyethylene.[1] Polyethylene has no functional groups that can provide crosslinking capability, such as the kind one finds in typical thermosetting resins. Hence, crosslinking must be induced by the incorporation of another component. The most common way is through the use of peroxide crosslinking agents added to the resin. Peroxides provide a source of free radicals when heated above their decomposition temperatures. These free radicals are capable of extracting a hydrogen from the polyethylene backbone, thus transferring the free radical site to the polyethylene. With this transfer accomplished, two polyethylene chains can be crosslinked. A second method of crosslinking polyethylene is by irradiation. In this case, the free radical formed on the polyethylene backbone is the result of electron beam irradiation. The third type of crosslinking is grafting of a silane onto the polyethylene and subsequently by the condensation reac-

tion of the silane graft with moisture. The method of making crosslinkable polyethylene by silane grafting followed by water crosslinking[1] has gained much attention in recent years because of its various advantages, such as easy processing, low cost, and capital investment, and favorable properties in the processed materials.

Thermal properties and crystal structures of crosslinked polyethylenes have been reported. Kao and Phillips[2] studied the effects of crosslinking density on many aspects of crystallization, including crystal structure, morphology, fusion, and crystallization kinetics for peroxide-crosslinked low-density polyethylene (LDPE). Turcsanyi and co-workers[3] investigated the effects of alkoxysilane grafting and subsequent network formation on the crystalline properties of polyethylene using differential scanning calorimetry (DSC). The mechanical properties and the crystallinity of the grafted and crosslinked samples were correlated. Kobayashi and co-workers[4] conducted DSC measurements of various peroxide-crosslinked polyethylenes of known thermal history and found close relationships between the DSC thermograms and the thermal history. Sen and co-workers[5] studied the effects of silane- and dicumyl peroxide-induced crosslinking and annealing on the thermal properties and structural parameters of polyethylene and its blends with ethylene propylene rubber using DSC and X-ray diffraction analysis. Crystallization and fusion behavior of the crosslinked polyethylene are markedly dependent on the sol (extractable) content and the effective network density of the gel.

Silane-grafted water-crosslinked LDPE is heterogeneous in molecular structure. This heterogeneous structure was demonstrated in our previous article[6] in which we reported the studies of thermal properties of both silane-grafted and silane-grafted water-crosslinked LDPE using DSC. The introduction of irregularities to the structure of LDPE by the silane grafts and the subsequent network formation led to multiple endothermic DSC thermograms. The multiple endothermic behavior is believed to be a result of heterogeneous structure of the sample. Because the final mechanical and thermal properties of the resulting materials are closely related to the heterogeneity of the samples, in this paper we follow up the previous finding[6] and study this multiple endothermic behavior in some detail using the thermal fractionation technique.

There have been a few methods developed to characterize molecular heterogeneity, including solvent–gradient elution fractionation (SGEF) and temperature-rising elution fractionation (TREF).[7–13] The TREF method is based on the crystallizability of sample by slow cooling from its dilute solution, followed by continuous elution with a simultaneous and fairly rapid rate of temperature rise. The SGEF method is based on the molecular weight of sample and is carried out by using solvent and nonsolvent mixtures with a variety of compositions. The drawback of these fractionation techniques is that they are time consuming and costly. Thus, DSC has been used as an alternative technique for thermal fractionation of polymers with heterogeneous molecular structure.[14–16] The DSC method is based on the same principle of separation as the TREF method, but it does not physically separate the fractions. With this DSC method, the sample is first melted and then annealed at various decreasing temperatures, starting from the melt to the totally crystallized solid. The melting behavior of the heat-treated sample is then analyzed by DSC. Using the DSC fractionation method, Adisson and co-workers[14] and Keating and co-workers[15] evaluated the comonomer distribution of linear LDPE and ethylene copolymers. Wolf and co-workers[16] used the DSC fractionation method to identify and distinguish between different types of LDPE. In this paper, the DSC fractionation method combined with regular DSC analysis, X-ray diffraction analysis, and polarized optical microscopy are used to characterize the heterogeneous molecular structure and morphology of the silane-grafted water-crosslinked LDPE.

EXPERIMENTAL

Materials

Silane-grafted LDPE was prepared by melt extrusion of LDPE with 0.05 phr (part of reagent per hundred parts of LDPE) of dicumyl peroxide, 1 phr of vinyl trimethoxysilane, and 0.05 phr of di-n-butyltin dilaurate. The extruder was operated at a speed of 20 rpm and at temperatures ranging from 170 °C at the feeding zone to 190 °C at the metering zone to 210 °C at the die zone of the extruder (single screw of 50 mm in diameter; L/D, 19; compression ratio, 3.5). LDPE (H0100) was received from Asia Polymer Corporation (Taipei, Taiwan) with a melt index (ASTM D1238) of 0.5 and a density (ASTM D1505) of 0.922 g/cm³. Dicumyl peroxide was used as an initiator for grafting reactions and supplied by Aldrich Chem-

ical Company (Milwaukee, WI). Vinyl trimethoxysilane was received from Tokyo Kasei Kogyo Company (Tokyo, Japan). Di-*n*-butyltin dilaurate was used as a catalyst for crosslinking reactions and received from Strem Chemicals (Newburyport, MA). The prepared silane-grafted LDPE film with thickness of ~1.0 mM was immersed into boiled water for 1 and 4 h to conduct crosslinking reactions. Degrees of crosslinking of the water-crosslinked samples were measured by determining the gel contents of the samples after extraction of the soluble component in the samples by decalin refluxing for 6 h. The gel contents determined were 30 and 70 wt % for 1 and 4 h of crosslinking, respectively.

Regular DSC Analysis

The melting behavior of six samples, including LDPE, silane-grafted LDPE (G-LDPE), and four silane-grafted water-crosslinked LDPE samples, was investigated by DSC (TA Instruments, New Castle, DE, DSC 2010). The silane-grafted water-crosslinked LDPE samples included samples from both before (XLPE1-30 and XLPE1-70) and after (XLPE2-30 and XLPE2-70) extraction by decalin (the numbers 30 and 70 denote 30 and 70 wt % gel content in the samples, respectively). DSC analysis was performed at a heating rate of 10 °C/min from 30 to 150 °C, and then cooled at various rates (5, 10, 15, and 20 °C/min) to 30°C and heated again at a rate of 10 or 40 °C/min to 150 °C to obtain the second set of endotherms. Integration of the endothermic peak area was performed with the software supplied by TA Instruments. The type of baseline for connecting the start and the end of the endothermic peak was the sigmoidal line, with horizontals at the start and the end of the peak.

Thermal Fractionation

The samples were heated under nitrogen in DSC from 30 to 150 °C at 10 °C/min, maintained at this temperature for 30 min, and then successively cooled by 5 °C at a rate of 1 °C/min. The specimens were maintained at each temperature for 30 min. Thus, the specimens were kept at each of the following temperatures for 30 min and then cooled to 30°C at 10 °C/min:145, 140, 135, 130, 125, 120, 115 ,110, 105, 100, 95 , 90, 85, 80, 75, 70, 65, and 60 °C. The samples were then heated again to 150 °C at 10 °C/min to obtain the second set of endotherms in which several peaks were obtained for each sample.

Wide-Angle X-ray Diffraction

The wide-angle X-ray diffraction patterns for polyethylene film samples were analyzed on a Siemens D5000 X-ray diffractometer operating at 40 kV and 35 mA, using molybdenum radiation with a wave length of 0.7093 Å as an X-ray source. Samples were mounted on a goniometer scanning at 1.2 °/min.

Polarized Optical Microscopy

Film samples prepared by casting from xylene were heated in a hot stage under nitrogen to 180 °C, held for 5 min, then cooled at a rate of 10 °C/min to 85 °C, and held again for 10 min. The treated samples were then transferred to a polarized optical microscope (POM, Zeiss D-07740) to observe their crystal morphologies. The samples characterized by POM included LDPE, G-LDPE, XLPE1-30, and XLPE1-50. XLPE1-50 was used instead of XLPE1-70 because the solution-cast XLPE1-50 film sample was easier to prepare.

RESULTS AND DISCUSSION

The DSC traces obtained from the second heating at a rate of 10 °C/min for six samples are shown in Figure 1. LDPE, G-LDPE, XLPE1-30, and XLPE2-30 give only one melting endotherm, with peak temperatures at 111.8, 110.9, 109.5, and 105.4 °C, respectively. From these melting temperatures, the effect of the silane grafting and subsequent network formation on the increasing of the structural irregularity of the sample appears to be the greatest in XLPE2-30 followed by XLPE1-30 and by G-LDPE. XLPE1-70 and XLPE2-70 give overlapped multiple endotherms. XLPE1-70 shows a sharp peak at ~125 °C, apparently corresponding to the melting of the molecular segments with low or no branching content. The 125 °C peak disappears for XLPE2-70 after extraction of the soluble component, which indeed includes molecules in a high structural regularity. This result suggests that the grafting reactions and the subsequent crosslinking reactions occur on those molecules with a low structural regularity; that is, those molecules with a high content of chain branching. This suggestion is consistent with the previous demonstration[17,18] that the grafting reactions occur at tertiary carbons of polyethylene molecules. The enthalpies of the endotherm in the 70–130°C range (Figure 1)
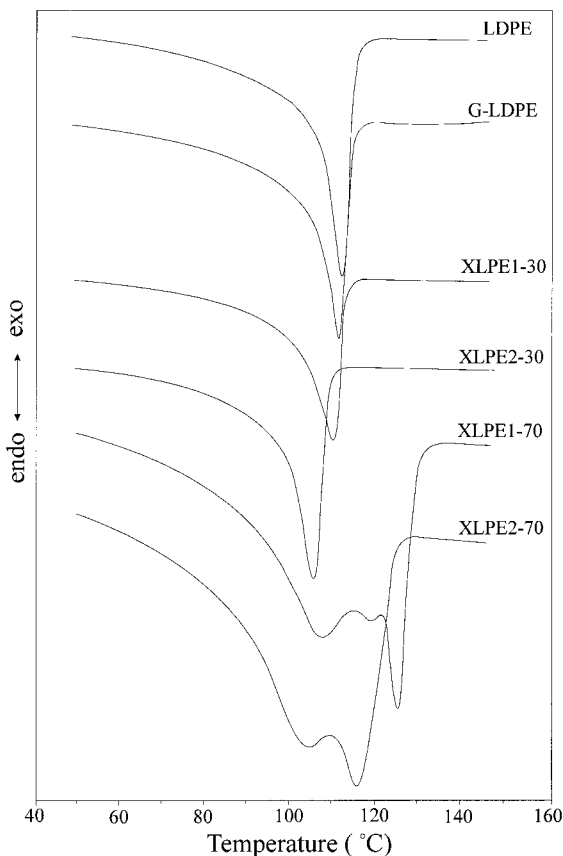
Figure 1 DSC traces obtained from the second heating scan at a rate of 10 °C/min for LDPE, G-LDPE, XLPE1-30, XLPE2-30, XLPE1-70, and XLPE2-70.

on the DSC curves obtained from the second heating scan at a rate of 40 °C/min as a function of the previous cooling rate. The melting enthalpy of LDPE decreases with increasing cooling rate and depends the most on the cooling rate of all six samples studied. This cooling rate dependence on the melting enthalpy is lessened for G-LDPE, followed by XLPE1-30 and XLPE2-30. The melting enthalpies of XLPE1-70 and XLPE2-70 surprisingly increase as the cooling rates increase, although these enthalpies are not significantly dependent on the cooling rates. The cause of the enthalpy increase with increasing cooling rate is perhaps a relatively high residual stress existing in the high gel fraction of samples after treating at a relatively high cooling rate. The DSC traces obtained from the second heating scan at a rate of 10 °C/min for XLPE1-70 as a function of the previous cooling rate are shown in Figure 3. The temperature of the sharpest peak in Figure 3
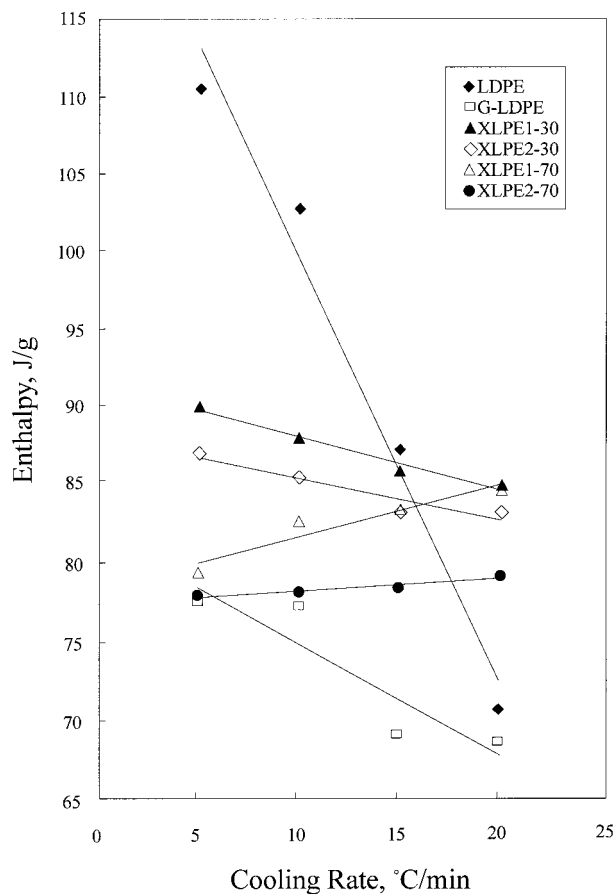
are 80.9, 73.8, 84.3, 73.2, 75.4, and 62.5 J/g for LDPE, G-LDPE, XLPE1-30, XLPE2-30, XLPE1-70, and XLPE2-70, respectively. As compared with LDPE, G-LDPE gives a decreased enthalpy due to an increase of irregularity in structure of the polymer caused by the silane graftings. XLPE1-30 gives increased enthalpies as compared with G-LDPE due to intermolecular crosslinkings. XLPE2-30 has lower melting enthalpy than XLPE1-30 due to removal of the sol fraction from the sample. The endothermic enthalpy, however, does not continue to increase with increasing gel fraction, as shown for XLPE1-70 and XLPE2-70. This result suggests that the irregularity of structure caused by network formation becomes significant as gel fraction increases. XLPE2-70 has lower melting enthalpy than XLPE1-70 due to the same reason as already described; that is, the removal of the sol component.

Plots are shown in Figure 2 of endothermic enthalpies of six samples between 70 and 130 °C

Figure 2 Endothermic enthalpies, from DSC analyses between 70 and 130 °C of the second heating curves at a rate of 40 °C/min, as functions of the previous cooling rates for six samples.

decreases slightly as the cooling rate is increased. As discussed previously, the sharpest peak for XLPE1-70 in Figure 3 is due to the melting of crystals with a high regularity in molecular structure. The shifting of the sharpest peak to the lower temperatures with increasing cooling rates indicates that the crystallization of the stereoregular molecules in XLPE1-70 decreases with increasing cooling rates due to the existing crosslinks.

In Figure 1, the broad endotherms for LDPE, G-LDPE, XLPE1-30, and XLPE2-30 imply an existence of heterogeneity in molecular structure, whereas the overlapped multiple endotherms for XLPE1-70 and XLPE2-70 suggest a high extent of heterogeneity in molecular structure for the polymers. The DSC traces of multiple melting endotherms for six samples that have been heat-treated in DSC according to the thermal fractionation method are shown in Figure 4. The multiple melting temperatures for these samples are listed in Table I. The multiple melting peaks in Figure 4 for each one of the samples demonstrate that every sample studied is heterogeneous in structure. The melting temperatures Tm1 to Tm6 are nearly identical for all six samples except XLPE2-30, with a missing peak at ~110 °C. In comparison, between XLPE1-30 and XLPE2-30, the missing peak for XLPE2-30 is due to the removal of the sol component in which the crosslinking is very low. The temperature of the largest peak of LDPE, G-LDPE, XLPE1-30, and XLPE2-30 in Figure 4 corresponds to the temperature of the only peak for the samples in Figure 1. As com-
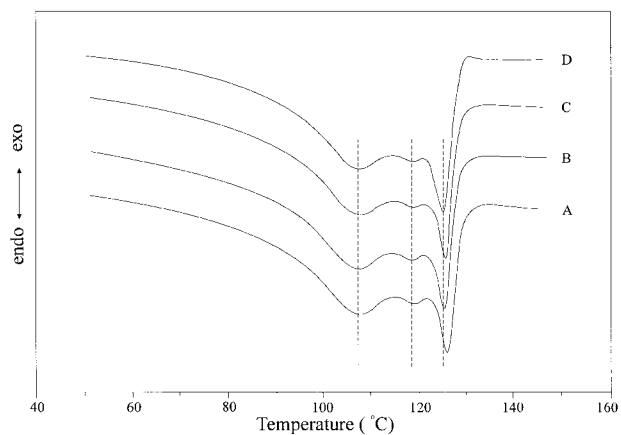

Figure 4 DSC traces at a heating rate of 10 °C/min for LDPE, G-LDPE, XLPE1-30, XLPE2-30, XLPE1-70, and XLPE2-70, which have been thermally fractionated in DSC.

Figure 3 DSC traces obtained from the second heating scan at a rate of 10 °C/min for XLPE1-70 as a function of the previous cooling rate at (A) 5 °C/min, (B) 10 °C/min, (C) 15 °C/min, and (D) 20 °C/min.
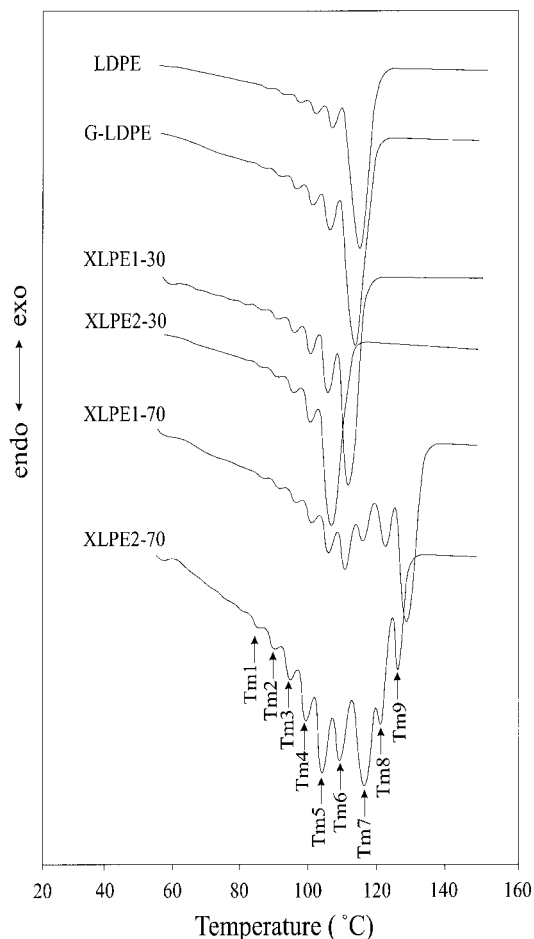
pared with XLPE1-30, the appearance at a relatively low temperature for the peak of XLPE2-30 in Figure 1 is caused by the removal of the sol component, not by the introduction of irregularity from the network formation. Peaks in Figure 4 at low temperatures (Tm1–Tm5, Table I) corresponds to various fractions of molecular structure in the component of gel (for crosslinked samples) or the component of branchings or graftings (for LDPE and G-LDPE) or both components. Each melting peak formed is representative of a distinct family of molecules with different structures. For XLPE1-70 and XLPE2-70, three additional melting peaks (Tm7–Tm9, Table I) are found at high temperatures. These three additional peaks are a result of splitting of the peak at ~112 °C, which is the peak temperature for G-LDPE, and indicate that the stereoregular frac-

Table I   Multiple Melting Temperatures for Six Polyethylene Samples Studied with DSC Thermal Fractionation

Polymer	Melting Temperature, °C								
	Tm1	Tm2	Tm3	Tm4	Tm5	Tm6	Tm7	Tm8	Tm9
LDPE	84.6	89.6	94.0	98.6	103.9	112.9	—	—	—
G-LDPE	84.4	88.6	93.9	98.4	103.4	111.9	—	—	—
XLPE1-30	83.9	88.4	93.1	97.9	103.1	109.4	—	—	—
XLPE2-30	83.4	88.9	93.4	98.4	104.9	—	—	—	—
XLPE1-70	83.9	89.1	93.9	98.9	104.1	108.9	113.9	120.9	127.4
XLPE2-70	83.9	88.9	93.6	98.4	103.3	108.6	116.2	120.4	125.2

tion of molecular structure has been excluded and its crystallization has been enhanced by the networked structure after crosslinking reactions. Examining the DSC trace of XLPE1-70 in Figure 4, the multiple peaks can be logically separated into two groups, including peaks at Tm1–Tm5 in one group and peaks at Tm6–Tm9 in the other. As discussed previously, the first group corresponds to molecules with a low structural regularity, whereas the second group at high temperatures corresponds to molecules with a high structural regularity. This hypothesis can be demonstrated by comparing the traces of XLPE1-70 and XLPE2-70. Peaks in the high temperature group are significantly changed after extraction treatment on the sample. For example, the peak at Tm9 is significantly reduced in XLPE2-70 due to the removal of the sol component with molecules in a high structural regularity. The splitting of the 112 °C peak into four peaks (Tm6–Tm9) for XLPE1-70 and XLPE2-70 represents that the chain length and branch in the samples are more diversified than those in LDPE, G-LDPE, XLPE1-30, and XLPE2-30. It is possible that the new nature of chain length or branched structure is created and exists in the sample after the reaction of crosslinking. This new nature of chain length or branched structure may involve a distribution of sequence length, giving different melting temperatures after thermal fractionation.

The X-ray diffraction patterns of LDPE, G-LDPE, XLPE1-70, and XLPE2-70 are shown in Figure 5. Because the unit cell of polyethylene is believed to be orthorhombic,[19] the diffraction angles (2θ) at ~9.7, 10.8, 16.4, 18.0, and 19.5° correspond to the set of planes of (110), (200), (120), (011), and (201), respectively. G-LDPE is similar to LDPE in the diffraction patterns. XLPE1-70 and XLPE2-70, however, show considerable changes in their diffraction patterns as compared with LDPE. The diffraction intensity at angle (2θ) of ~l9.7° for XLPE1-70 appears, as compared with that of LDPE or G-LDPE, to be significantly
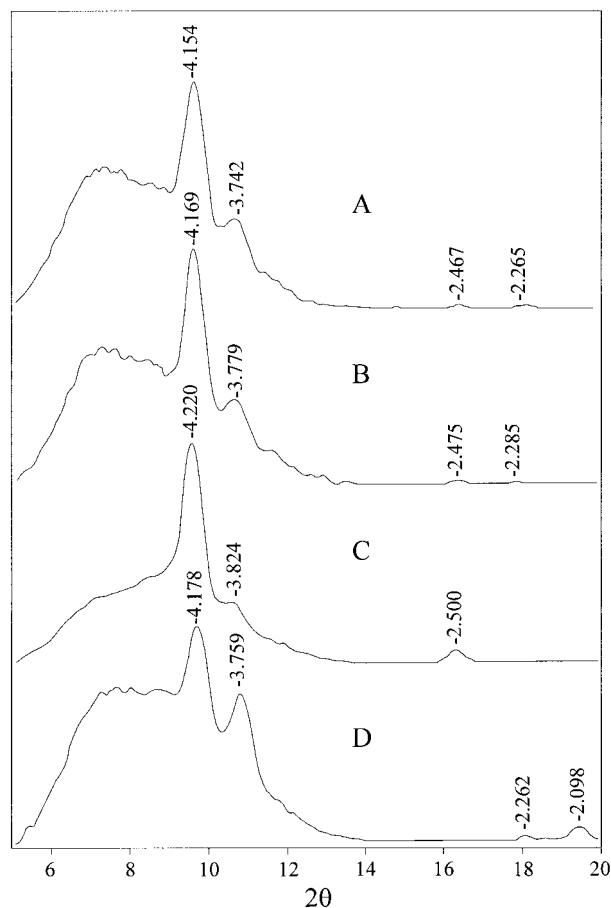

Figure 5   X-ray diffraction patterns for (A) LDPE, (B) G-LDPE, (C) XLPE1-70, and (D) XLPE2-70. The number at the top of a peak denotes the spacing distance of a set of diffraction planes.

Table II   Lattice Constants of the Orthorhombic Unit Cell and Calculated Densities of the Unit Cell for Various Polyethylene Samples

Sample	Lattice Constant, Å			Calculated Density, g/cm^3
	a	b	c	
Literature data[a]	7.4	4.93	2.54	1.004
LDPE	7.484	4.994	2.541	0.979
G-LDPE	7.558	5.002	2.569	0.957
XLPE1-70	7.648	5.074	2.546	0.941
XLPE2-70	7.518	5.026	2.533	0.971

[a] Reference 19.

increased, which is an indication that the crystallization of XLPE1-70 has been enhanced. The diffraction intensity at the same angle for XLPE2-70 appears, as compared with that of XLPE1-70, to be significantly reduced due to the removal of the sol component with molecules in a high structural regularity. Thus, the X-ray diffraction data are consistent with the DSC data, as previously shown and discussed. The appearance of the diffraction line at 19.5° for XLPE2-70 demonstrates that a new nature of chain length or branch structure is created and exists in the sample as a result of crosslinking reactions. Further experiments will be needed to resolve this point.

The diffraction angle or the d_{hl} value (shown at the top of a peak) in Figure 5 of a diffraction peak is not the same for all four samples studied. By applying the Bragg equation and considering the perpendicular distance between adjacent planes with indices (hkl) as $d_{hkl} = (h^2/a^2 + k^2/b^2 + l^2/c^2)^{-1/2}$, lattice constants (a, b, and c) of the orthorhombic unit cell can be calculated. From these lattice constants, the densities of samples can be determined by assuming that there are four CH_2 groups per unit cell.[20] Lattice constants of the orthorhombic unit cell and the calculated densities of the unit cell of samples are listed in Table II.

From Figure 5, the d_{110} values for LDPE, G-LDPE, XLPE1-70, and XLPE2-70 are 4.154, 4.169, 4.220, and 4.178 Å, respectively. The spacing for the (110) planes of sample appears to increase after the sample has been grafted with the silane and crosslinked by water, but then decrease after the extraction of the sol component from the crosslinked sample. Similar results are obtained for the spacings of the (200) planes for

the samples. This result is caused by the introduction of irregularity into the structure of the sample by the silyl trimethoxy groups in G-LDPE and by the subsequent crosslinking of these groups in XLPE1-70. The increasing in the values of a and b of the unit cell and the decreasing of the calculated density of the unit cell (Table II) for G-LDPE and XLPE1-70, as compared with that for LDPE, also provide evidence that irregularity has been introduced into the sample. Examining the c values of the unit cells of samples, G-LDPE shows a higher value than does LDPE. This difference suggests that the silane grafts have caused changes, to some extent, in the conformation of the molecules from the zigzag form (carbon—carbon bonds are *trans*) to the *gauche* form. This conformational change is found to a lesser extent for XLPE1-70 than for G-LDPE. As compared with XLPE1-70, XLPE2-70 has lower values for all three lattice constants and thus a higher value of calculated density. The reason for this difference is the effect of intermolecular contraction in XLPE2-70 after the sol component trapped in the gel component in the sample is removed.

The polarized optical micrographs for LDPE, G-LDPE, XLPE1-30, and XLPE1-50 are shown in Figure 6. Crystal formations can be seen from these micrographs for all four samples studied. Because samples for the POM characterization are prepared by casting from xylene, crystal morphologies as exhibited in polarized optical micrographs for LDPE and G-LDPE represent morphologies of the bulk of these samples due to complete dissolution of samples in xylene at elevated temperature. Morphologies as exhibited in the micrographs for XLPE1-30 and XLPE1-50, however, represent morphologies of only the soluble component of the samples in xylene. As can be seen from micrograph A in Figure 6 for LDPE, there are many spherulites with varied sizes impinging on each other. The silane-grafted LDPE results in much decreased spherulite size, with much less perfection (micrograph B in Figure 6). This result suggests that the silane grafts, on the one hand, act as a nucleating agent in crystallization of G-LDPE, leading to a decreased spherulite size, and, on the other hand, introduce structural irregularity into LDPE molecules, leading to low perfection in the growth of spherulite. The size of spherulite increases with increasing degree of crosslinking, as can be seen from micrographs C and D in Figure 6. The size of spherulite for the sol component of XLPE1-50 is even bigger
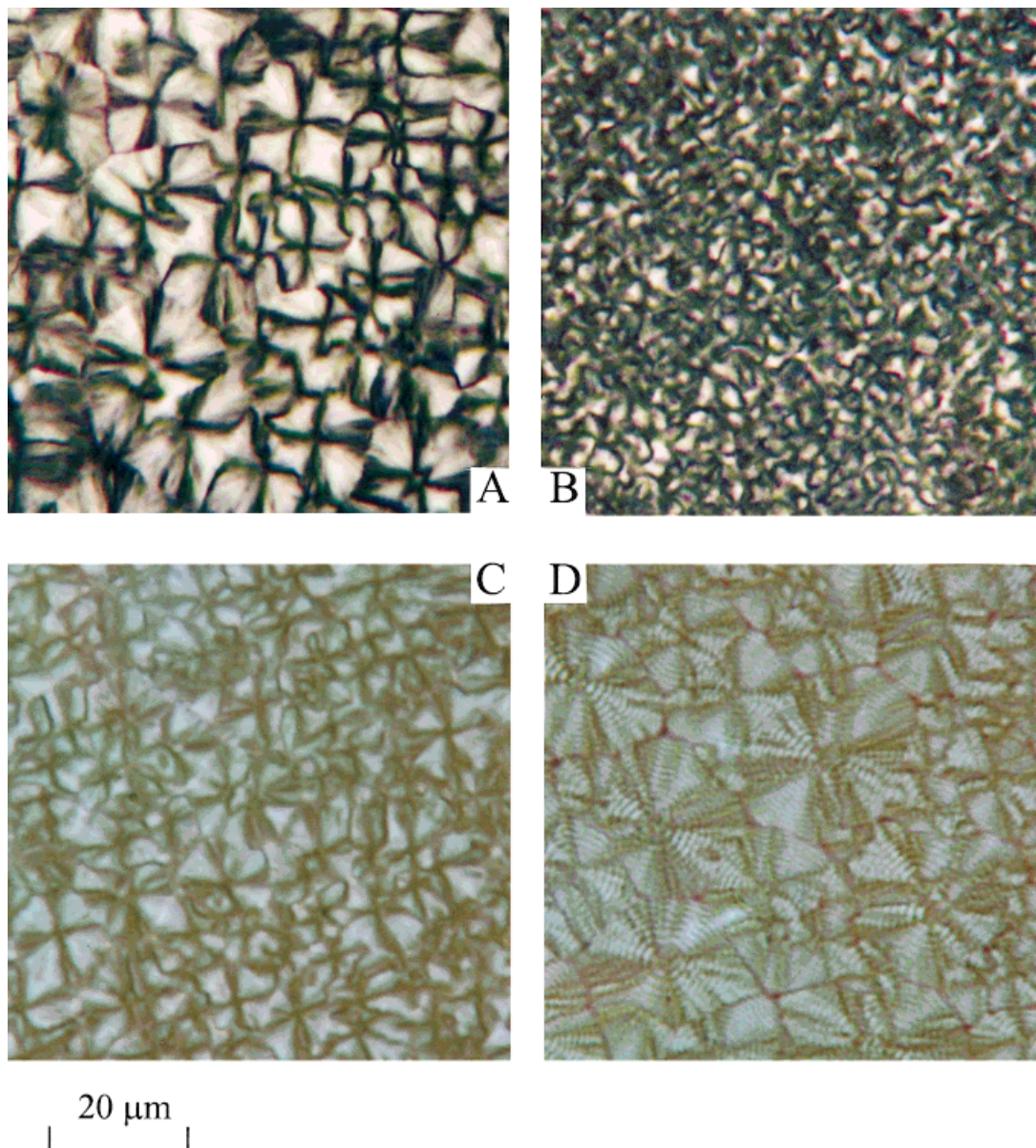
Figure 6 Polarized optical micrographs for (A) LDPE, (B) G-LDPE, (C) XLPE1-30, and (D) XLPE1-50. [Color figure can be viewed in the online issue, which is available at www.interscience.wiley.com.]

than that for LDPE. This difference suggests that the regularity of the sol components in these samples increases with increasing degree of crosslinking because, as previously discussed, the silane grafting reactions (and thus crosslinking reactions) occur mostly with those molecules with branches (i.e., molecules with tertiary carbons). As degree of crosslinking increases, the content of molecules with branches or silane grafts (or the content of molecules with a low structural regularity) decreases in the sol component in the sam-

ple. In other words, the concentration of molecules with low content of branches or silane grafts in the sol component in the sample increases with increasing degree of crosslinking. The POM micrographs in Figure 6 can thus explain the finding of crystallization enhancement on silane grafting and crosslinking of LDPE as demonstrated from DSC data. XLPE1-50, as shown in micrograph D, exhibits a significantly different morphological pattern from other samples studied. This special pattern in micrograph D is normally seen from

high-density polyethylene, which has a very low content of branches. Therefore, the POM data confirm that the silane is mostly grafted onto the tertiary carbons on polyethylene molecules.

CONCLUSIONS

LDPE, silane-grafted LDPE (G-LDPE), and silane-grafted water-crosslinked LDPE are heterogeneous in their molecular structures, as demonstrated by regular DSC analyses in which these samples give either one broad endothermic peak or overlapped multiple endothermic peaks in a much broader temperature range. These molecules with heterogeneous molecular structures can be thermally fractionated by DSC. After thermal fractionation in the range 60–145 °C, LDPE, G-LDPE, and the low gel fraction (30 wt %) of crosslinked samples give five to six endothermic peaks in the low-temperature range, whereas the high gel fraction (70 wt %) of samples gives nine peaks, with the three additional peaks appearing in the high-temperature range. These multiple peaks correspond to fractions of different molecular structures, with the additional peaks for the high gel fraction samples corresponding to fractions of structurally regular molecules in the sol component of samples. With increasing gel fraction, the fraction of structurally regular molecules in the sol component increases and crystallization of the sol component is thus enhanced. This crystallization enhancement behavior is supported by the X-ray diffraction data and polarized optical micrographs.

REFERENCES

1. Scott, H.G. U.S. Pat. 3,646,155 (1972).
2. Kao, Y.H.; Phillips, P.J. Polymer 1986, 27, 1669.
3. Turcsanyi, B.; Fekete, E.; Pukanszky, B.; Tabor, I. J Therm Anal 1990, 36, 1775.
4. Kobayashi, K.; Nakayama, S.; Niwa, T. Intern J Polymeric Mater 1993, 21, 147.
5. Sen, A.K.; Mukherjee, B.; Bhattacharyya, A.S.; De, P.P.; Bhowmick, A.K. J Therm Anal 1993, vol. 39, 887.
6. Shieh, Y.T.; Hsiao, K.I. J Appl Polym Sci 1998, 70, 1075.
7. Hosoda, S. Polym J 1988, 20(5), 383–397.
8. Wild, L.; Ryle, T.R.; Knobeloch, D.C.; Peat, I.R. J Polym Sci: Polym Phys Ed 1982, 20, 441–455.
9. Feng, Y.; Jin, X.; Hay, J.N. Polym J 1998, 30, 215.
10. Shirayama, K.; Okada, T.; Kita, S. J Polym Sci, A-2 1965, 3, 907.
11. Shirayama, K.; Kita, S.; Watabe, H. Makromol Chem 1972, 151, 97.
12. Wijga, P.W.O.; van Schooten, J.; Boerma, J. Makromol Chem 1960, 36, 115.
13. Nakajima, A.; Fujiwara, H. Bull Chem Soc Jpn 1964, 37, 909.
14. Adisson, E.; Ribeiro, M.; Deffieux, A.; Fontanille, M. Polymer 1992, 33(20), 4337–4342.
15. Keating, M.Y.; McCord, E.F. Thermochim Acta 1994, 243,129–145.
16. Wolf, B.; Kenig, S.; Klopstock, J.; Miltz, J. J Appl Polym Sci 1996, 62, 1339–1345.
17. Shieh, Y.T.; Tsai, T.H. J Appl Polym Sci 1998, 69, 255.
18. Shieh. Y.T.; Liu, C.M. J Appl Polym Sci 1999, 74, 3404.
19. Kakudo, M.; Ullman, R. J Polym Sci 1960, 45, 91.
20. Sperling, L.H. Introduction to Physical Polymer Science, 2nd edition; John Wiley & Sons, Inc.: New York, 1992.